

Supplementary Materials: Ivabradine Hydrochloride (S)-Mandelic Acid Cocrystal: In Situ Preparation during Formulation

Veronika Sládková, Ondřej Dammer, Gregor Sedmak, Eliška Skořepová and Bohumil Kratochvíl

I. Solid-State Characterization of Ivabradine Hydrochloride (S)-Mandelic Acid 1:1 Cocrystal (ICISM)

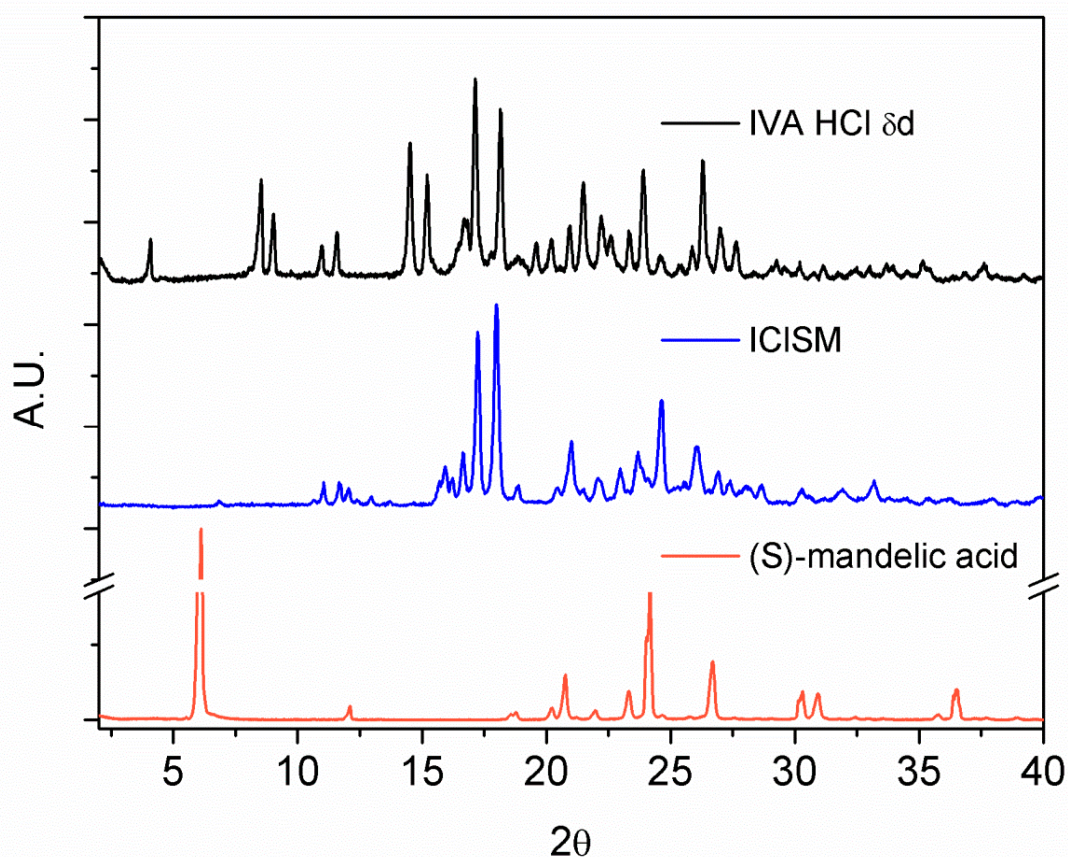


Figure S1. The XRPD patterns of co-crystal ICISM (**middle**, blue); starting components, ivabradin hydrochloride form δd (**top**, black); and (S)-mandelic acid (**bottom**, orange).

The powder pattern of (S)-mandelic acid was preferentially oriented, therefore, for clarity purposes, in the figure the first peak is displayed with a break.

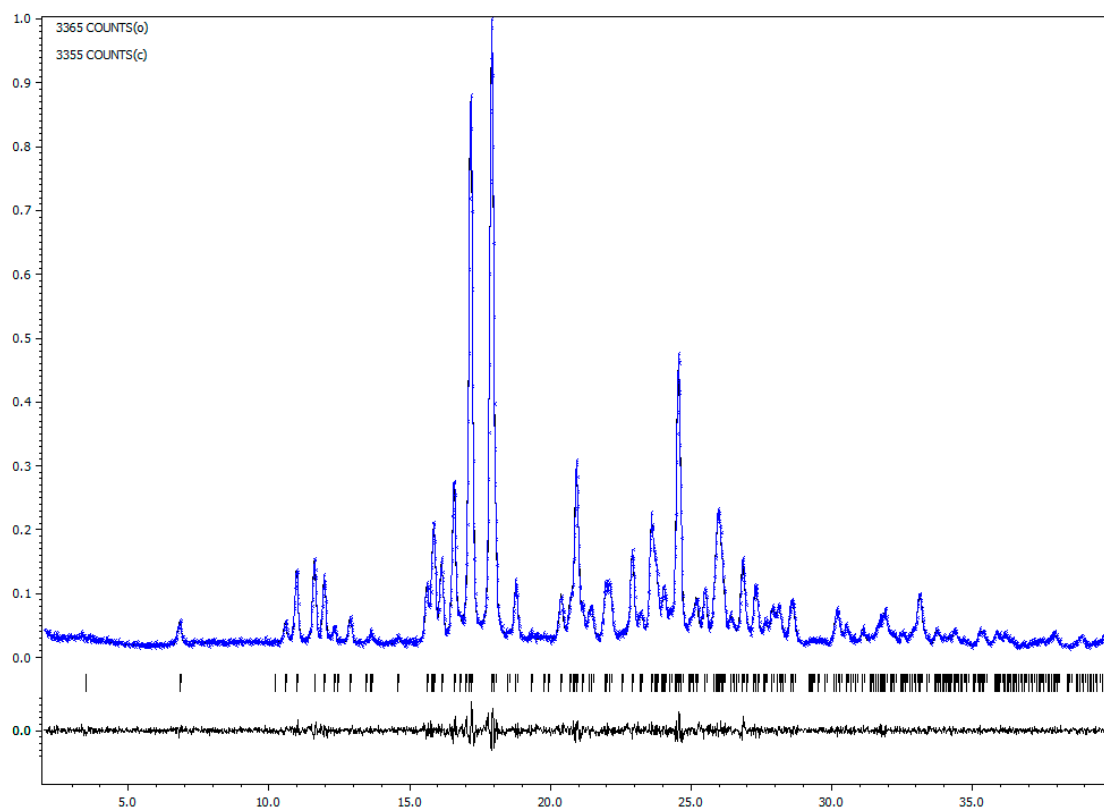


Figure S2. The final Rietveld plot of the co-crystal ICISM, showing the measured and the calculated data. The calculated Bragg positions are shown by vertical bars.

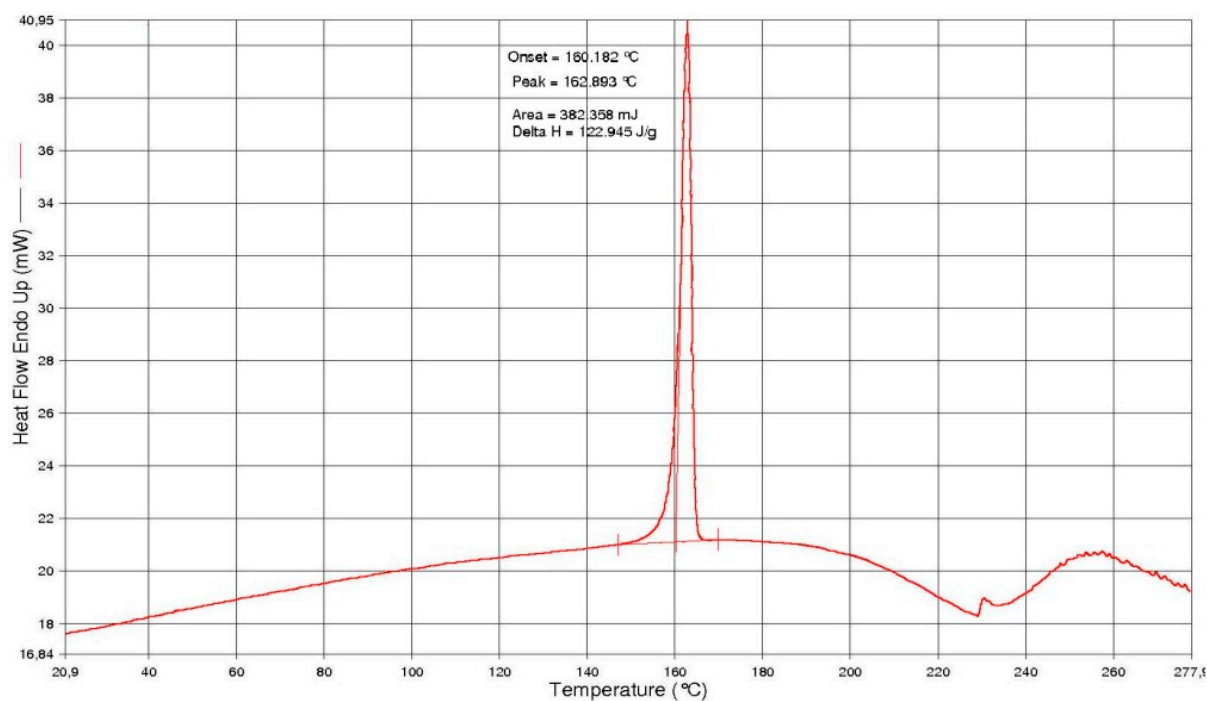


Figure S3. The DSC curve of the co-crystal ICISM.

The major endotherm is $T_{\text{onset}} = 160.2\text{ °C}$ (162.9 °C at maximum). The melting temperatures of the input components are different: (*S*)-mandelic acid $T_{\text{onset}} = 131.8\text{ °C}$ (134.3 °C at maximum); ivabradine hydrochloride $T_{\text{onset}} = 194.7\text{ °C}$ (196.7 °C at maximum).

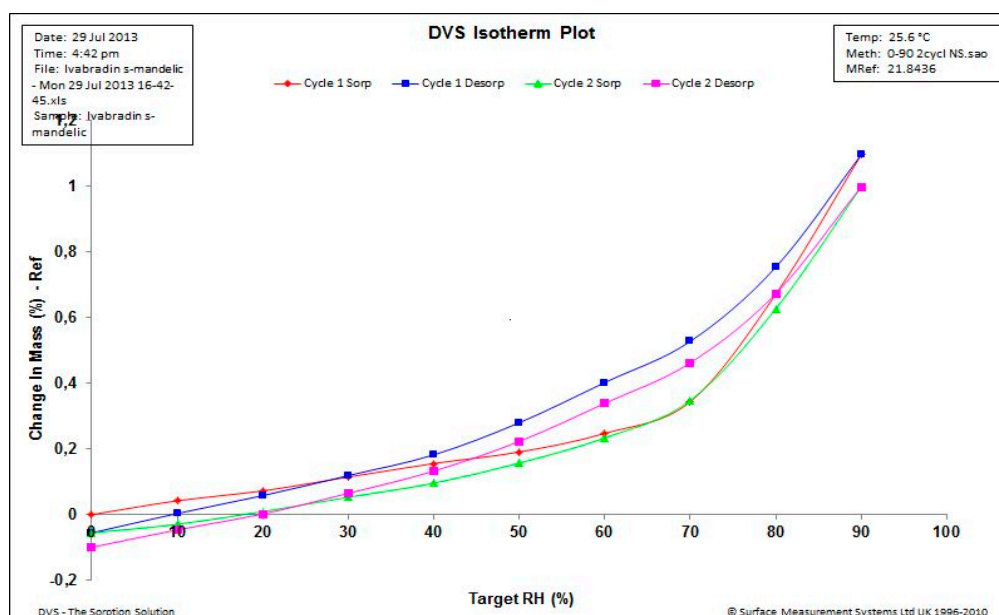


Figure S4. The DVS curve of the co-crystal ICISM.

The sample of ICISM was measured in two cycles of 0-90-0% relative humidity (RH). At 90% RH, the sample increased its weight by 1.1% due to water vapor sorption. During the subsequent desorption the sample returned to its starting weight, the whole process appearing to be reversible. The first cycle is identical to the second one. The ICISM co-crystal is weakly hygroscopic.

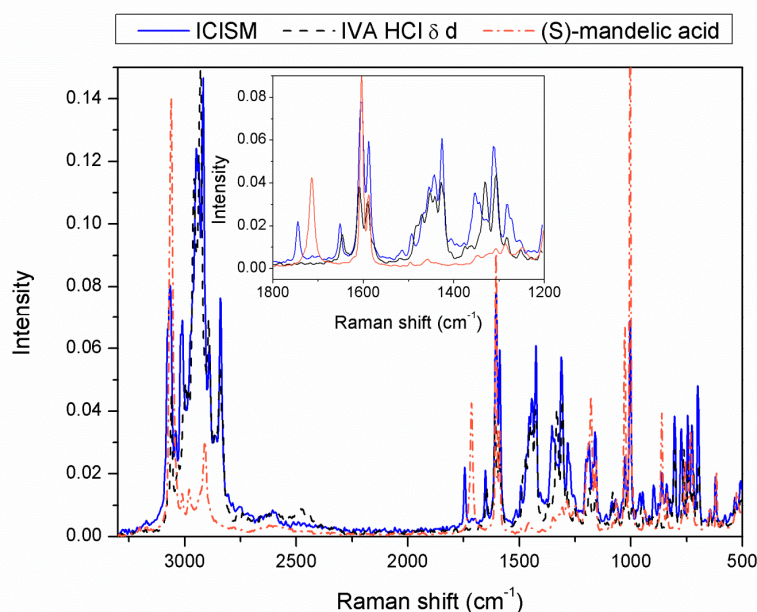


Figure S5. The Raman spectra of ICISM (blue curve), ivabradine hydrochloride δd (black dashed curve), and (S)-mandelic acid (orange dash dotted curve).

The measured spectrum of co-crystal ICISM is not a mere sum of spectra of the input components ivabradine hydrochloride and (S)-mandelic acid and, thus, is not a simple physical mixture. The observed changes in the spectrum can be ascribed to the newly created interactions between ivabradine hydrochloride and (S)-mandelic acid. The most significant is the shift of the vibration of (S)-mandelic acid carbonyl by 30 cm^{-1} towards a higher wavenumber and the changes of C-H vibrations in the vicinity of quaternary nitrogen. The observed changes are related to the occurrence of a new phase.

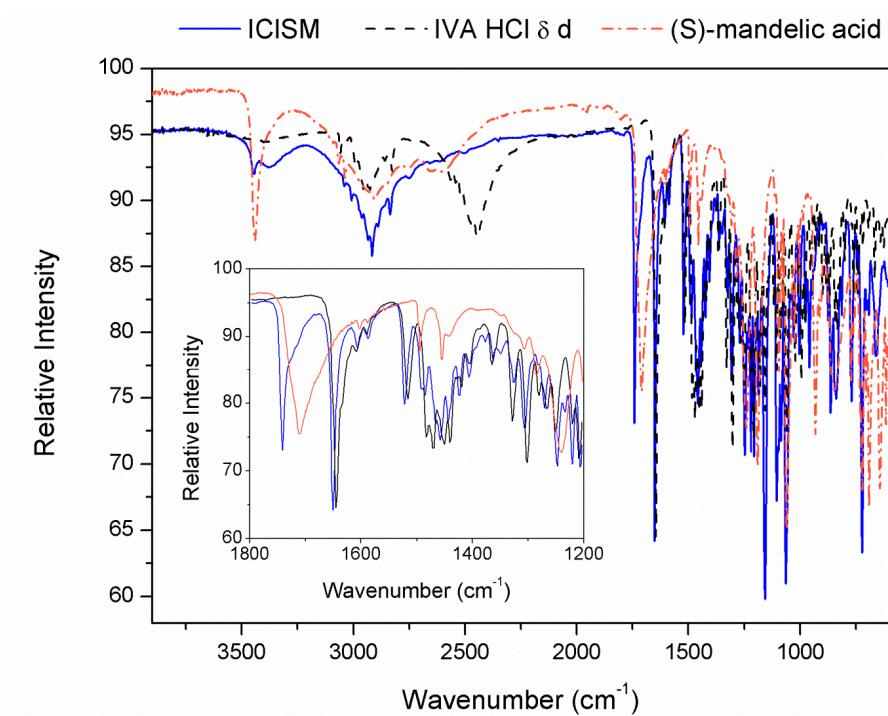


Figure S6. The infrared (IR) spectra of ICISM (blue curve), ivabradine hydrochloride $\delta\delta$ (black dashed curve), and (*S*)-mandelic acid (orange dotted curve).

The IR spectrum of the co-crystal ICISM is also not a mere sum of the input components' spectra, similarly to the Raman spectrum. The observed changes in the spectrum of (*S*)-mandelic acid are: (i) the shift of the carbonyl band of the carboxyl group towards higher wavenumber, and (ii) a decrease in the intensity of vibrations at 3500 cm^{-1} assigned to the secondary alcohol. Furthermore, the vibration intensity of the N-H^+ functional group of the hydrochloride at 2500 cm^{-1} changed, which corresponds to the newly-established interaction between ivabradine hydrochloride and (*S*)-mandelic acid.

Table S1. Comparison of long-term ($25\text{ }^{\circ}\text{C}/60\% \text{RH}$) and accelerated ($40\text{ }^{\circ}\text{C}/75\% \text{RH}$) physical stability of ICISM co-crystal and polymorphic form $\delta\delta$.

	2 weeks	1 month	3 months
Cocrystal ICISM			
$25\text{ }^{\circ}\text{C}/60\% \text{RH}$	No change	No change	No change
$40\text{ }^{\circ}\text{C}/75\% \text{RH}$	No change	No change	No change
IVA HCl $\delta\delta$			
$25\text{ }^{\circ}\text{C}/60\% \text{RH}$	No change	Traces of form δ	δ
$40\text{ }^{\circ}\text{C}/75\% \text{RH}$	No change	Traces of form α	Mixture of δ and α

The co-crystal and form $\delta\delta$ were treated for two weeks, one month, and three months at $25\text{ }^{\circ}\text{C}/60\% \text{RH}$ and $40\text{ }^{\circ}\text{C}/75\% \text{RH}$ and analyzed by XRPD. The studies showed that the co-crystal ICISM remained stable in contrast with IVA HCl form $\delta\delta$, which, after one month contained polymorphic impurities, such as form δ and α .

Table S2. Characterization (pH, water content, solid form (XRPD), chemical purity (UPLC)) of formulation mixtures A–C, containing ICISM co-crystal.

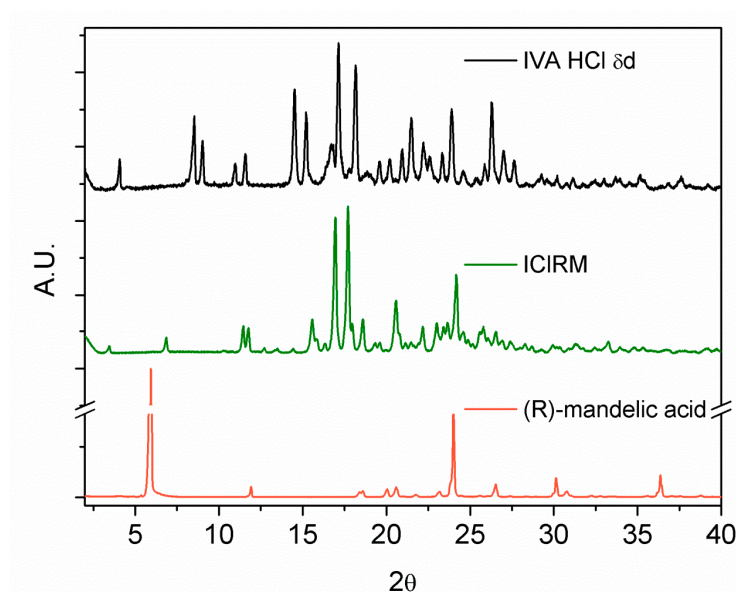
	A	B	C
pH	3.7	3.7	6.9
Water content	4.41	0.30	4.28
	<i>Sum of chemical impurities (%)</i>		
start	0.06	0.00	0.12
72h 80 °C N2	0.05	0.26	1.91
72h 80 °C atm.	0.12	0.14	1.70
	<i>Physical (phase) impurities</i>		
start	ICISM	ICISM	ICISM
72h 80 °C N2	admix.γ form	admix.γ form	ICISM
72h 80 °C atm.	admix.γ form	admix.γ form	ICISM

Table S3. Characterization of formulation mixtures D–J.

	D	E	F	G	H	I	J
pH	3.6	3.6	4.8	4.0	7.4	3.5	3.1
Water content	4.26	0.13	4.25	4.26	4.22	4.45	4.47
	<i>Sum of chemical impurities (%)</i>						
start	0.12	0.12	0.14	0.12	0.06	0.14	0.14
72h 80 °C N2	0.12	0.25	0.14	1.98	8.84	0.14	0.87
72h 80 °C atm.	0.13	0.22	0.31	2.48	9.23	0.14	0.75
	<i>Physical (phase) impurities</i>						
start	ICISM	ICISM	ICISM	ICISM	ICISM	ICISM	ICISM
72h 80 °C N2	admix.γ form	ICISM	admix.γ form	admix.γ form	admix.γ form	ICISM	ICISM
72h 80 °C atm.	admix.γ form	ICISM	admix.γ form	admix.γ form	admix.γ form	ICISM	ICISM

The mixtures were treated for 72 h at 80 °C under ambient and inert (nitrogen) atmosphere and physical and chemical stability were checked.

II. Solid-State Characterization of Ivabradine Hydrochloride (R)-Mandelic Acid 1:1 Co-Crystal (ICIRM)

**Figure S7.** The XRPD patterns of co-crystal ICIRM (middle, green); starting components, ivabradine hydrochloride form δd (top, black); and (R)-mandelic acid (bottom, orange).

The powder pattern of (*R*)-mandelic acid was preferentially oriented, therefore, for clarity purposes, in the figure the first peak is displayed with a break.

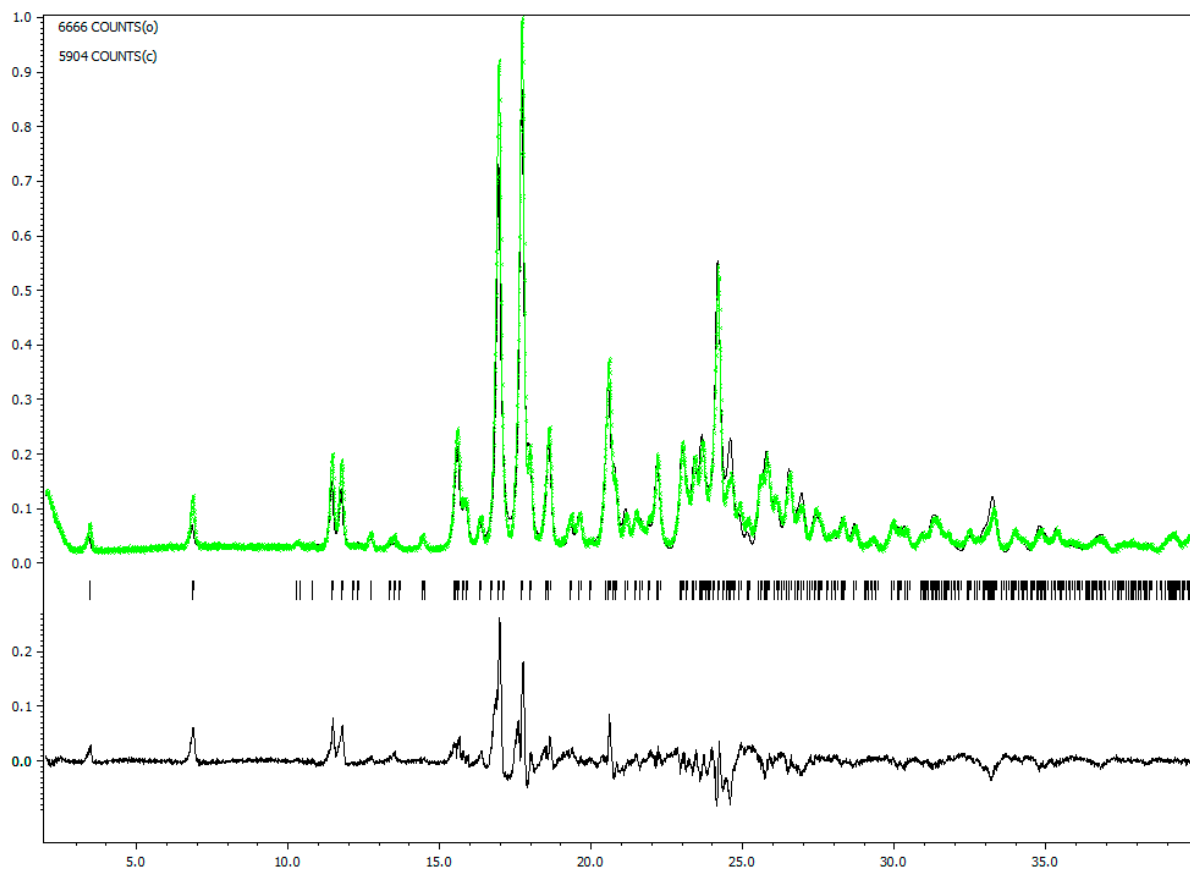


Figure S8. The final Rietveld plot of the co-crystal ICISM, showing the measured and the calculated data.

The calculated Bragg positions are shown by vertical bars. The fit is not very good due to different intensities, but all of the peaks are explained and the powder does not contain any phase impurities.

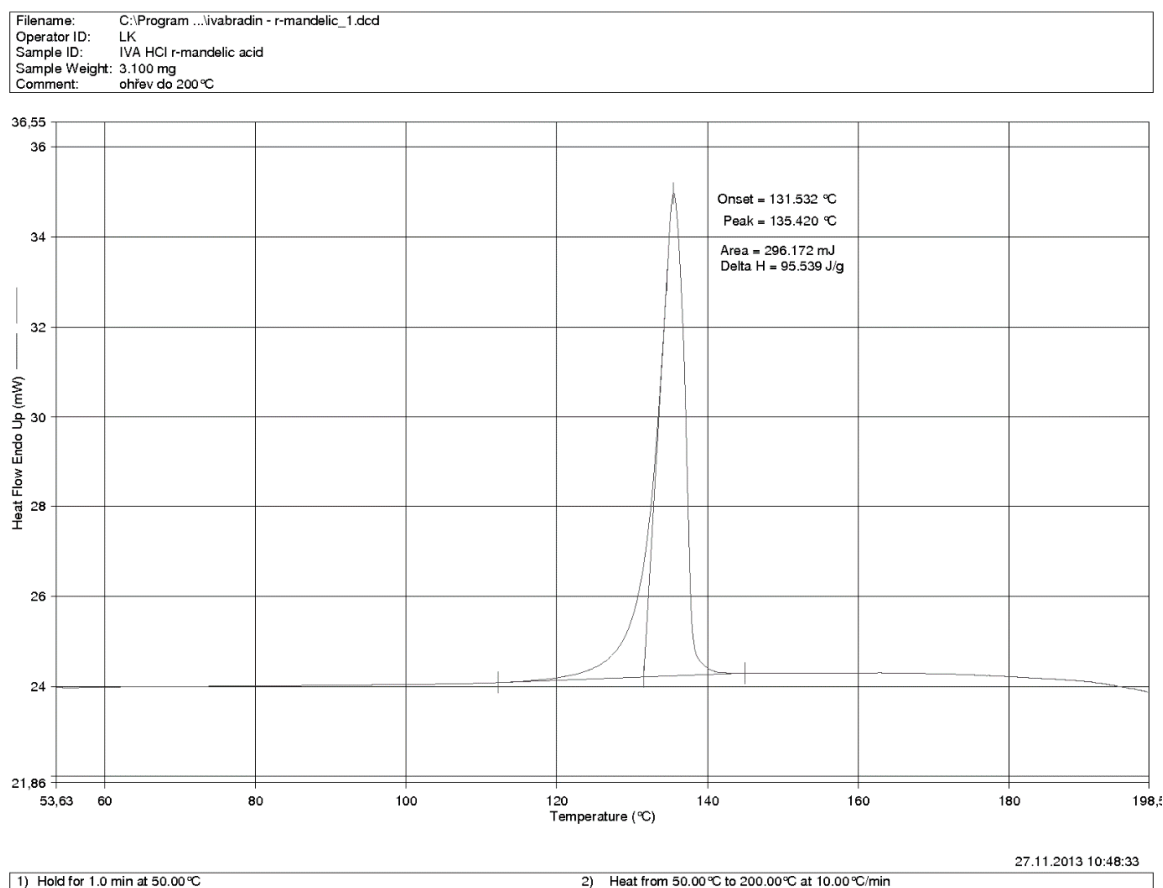


Figure S9. The DSC curve of the co-crystal ICIRM.

The major endotherm is $T_{onset} = 131.5 \text{ °C}$ (135.4 °C at maximum).

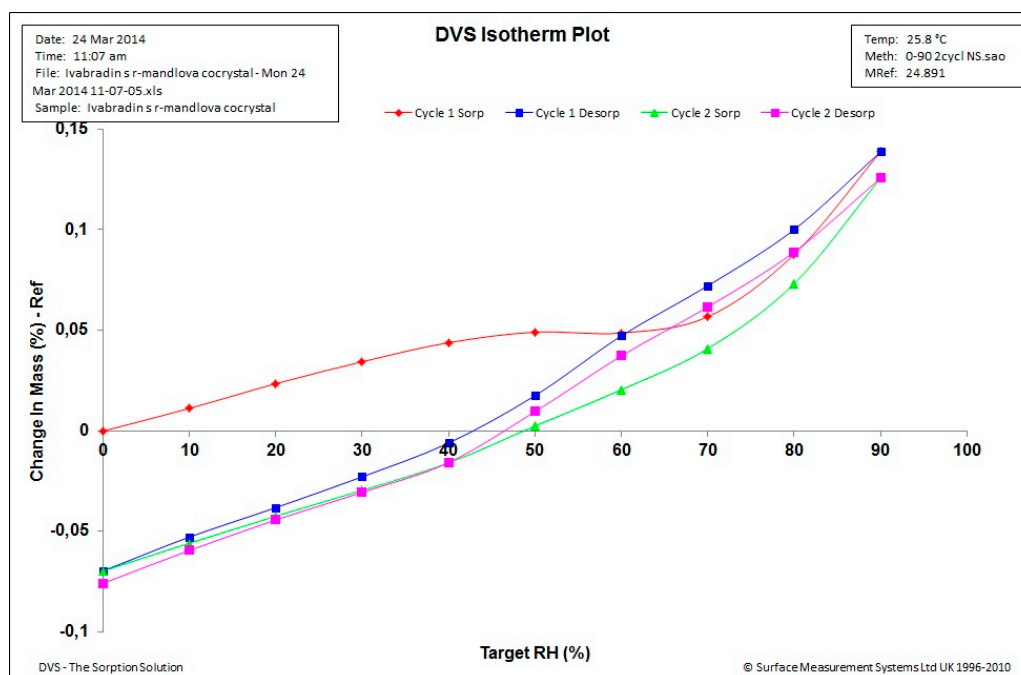


Figure S10. The DVS curve of the co-crystal ICIRM.

At 90% RH, the sample weight increased by 0.15% due to water vapor sorption. During the subsequent desorption the sample lost more weight than it gained during the adsorption, which was possibly caused by the residual humidity of the input sample. The co-crystal is not hygroscopic.

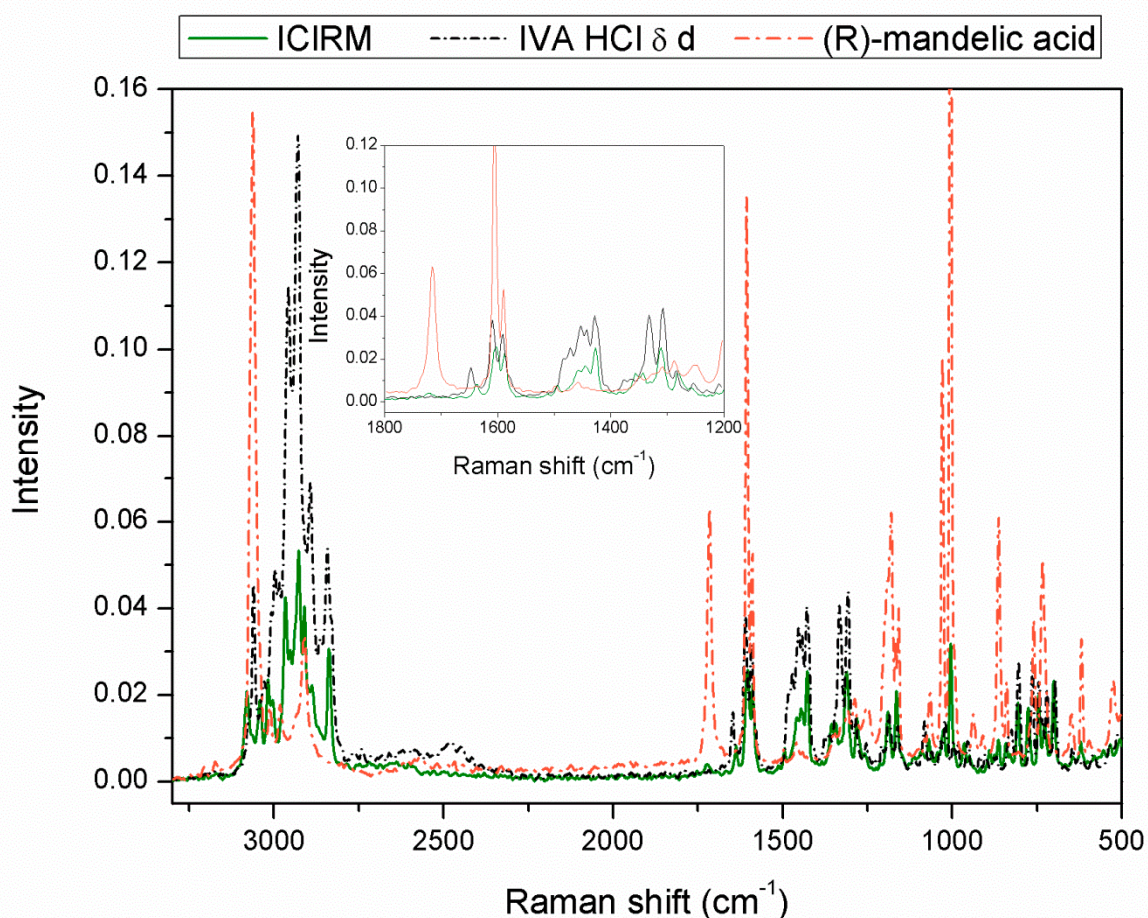


Figure S11. The Raman spectra of ICIRM (green curve), ivabradine hydrochloride δd (black dashed curve), and (*R*)-mandelic acid (orange dotted curve).

The measured spectrum of the cocrystal ICIRM is not a mere sum of the spectra of the input components ivabradine hydrochloride and (*R*)-mandelic acid and, thus, it is not a simple physical mixture. The observed changes in the co-crystal spectrum can be assigned to newly formed interactions between ivabradine hydrochloride and (*R*)-mandelic acid. Shifts of the vibrations of the (*R*)-mandelic acid carbonyl towards lower wavenumber values, and of ivabradine hydrochloride carbonyl towards lower wavenumber values, and changes of C-H deformation vibrations of ivabradine around 1450 cm⁻¹ are the most significant. The observed changes are related to the occurrence of a new phase.

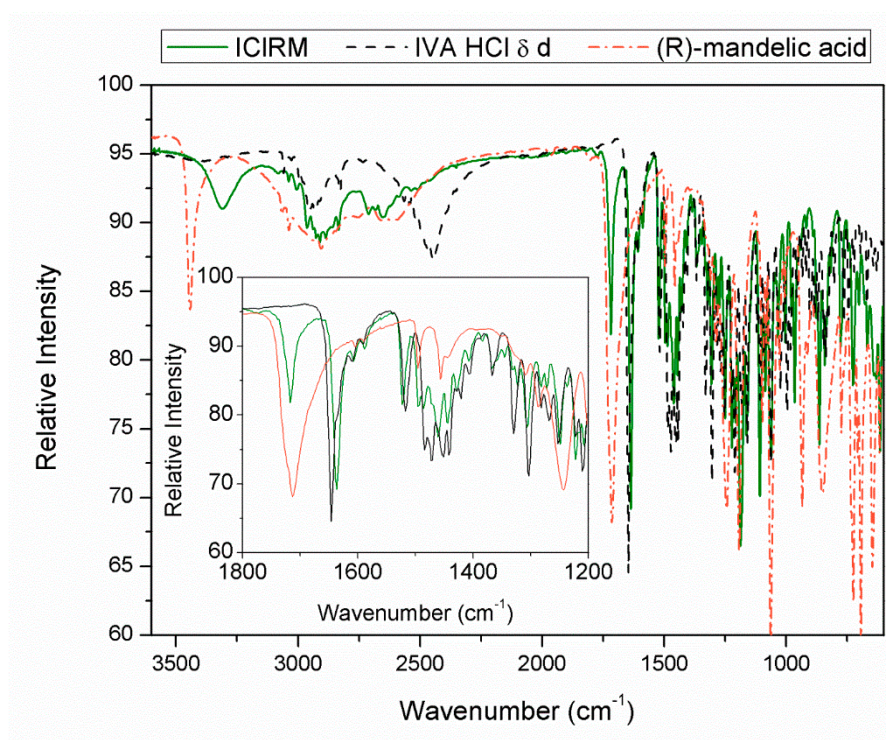


Figure S12. The IR spectra of ICIRM (green curve), ivabradine hydrochloride δd (black dashed curve), and (*R*)-mandelic acid (orange dotted curve).

As in the Raman spectrum, the IR spectrum of the co-crystal ICIRM is also not a mere sum of spectra of the input components ivabradine hydrochloride and (*S*)-mandelic acid and, thus, is not a simple mixture. The changes of (*R*)-mandelic acid are observed: (i) changes in the range of valence vibrations of the -OH groups around 3000 cm^{-1} , (ii) the changes of the deformation vibrations of the hydroxy groups in the area of 1400 cm^{-1} , and (iii) a shift of the vibration band of the carbonyl of the carboxylic group of mandelic acid towards higher wavenumbers and that of the ivabradine hydrochloride carbonyl towards lower wavenumbers. Furthermore, the vibration intensity of the N-H⁺ functional group of the hydrochloride at 2500 cm^{-1} changes, which corresponds to the newly-formed interaction between ivabradine hydrochloride and (*R*)-mandelic acid.

III. Comparison of ICISM and ICIRM

The XRPD patterns, IR and Raman spectra of ICISM (blue) and ICIRM (green) are displayed. The powder patterns are similar, as both unit cell parameters and structures of ICISM and ICIRM are very similar. The differences in the IR and Raman spectra are more pronounced and correspond to the different interactions between mandelic acid functional groups with ivabradine hydrochloride. These interactions are apparent when viewing the structures obtained from single-crystal X-ray diffraction data.

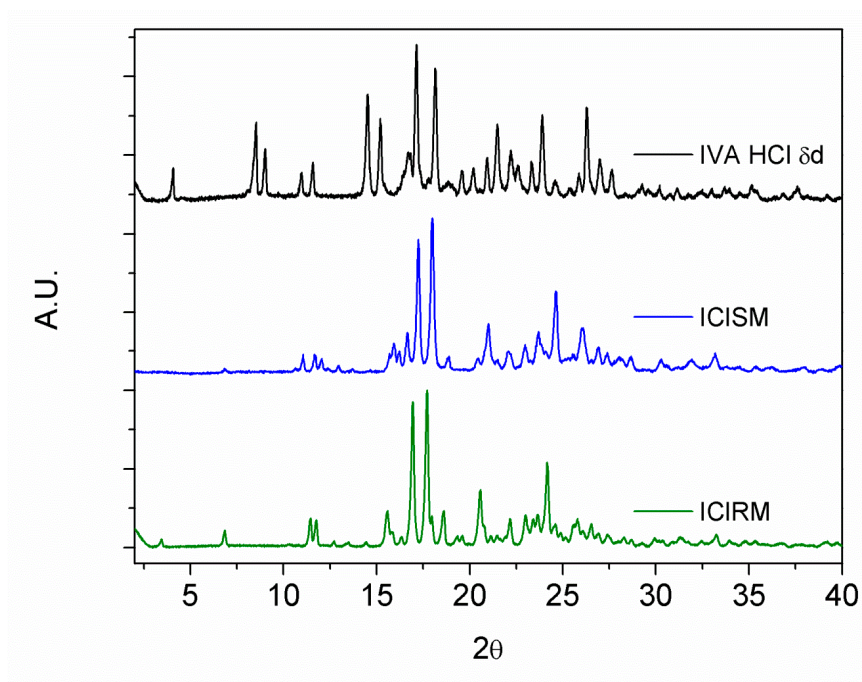


Figure S13. The XRPD patterns of IVA HCl δd (black), ICISM (blue) and ICIRM (green).

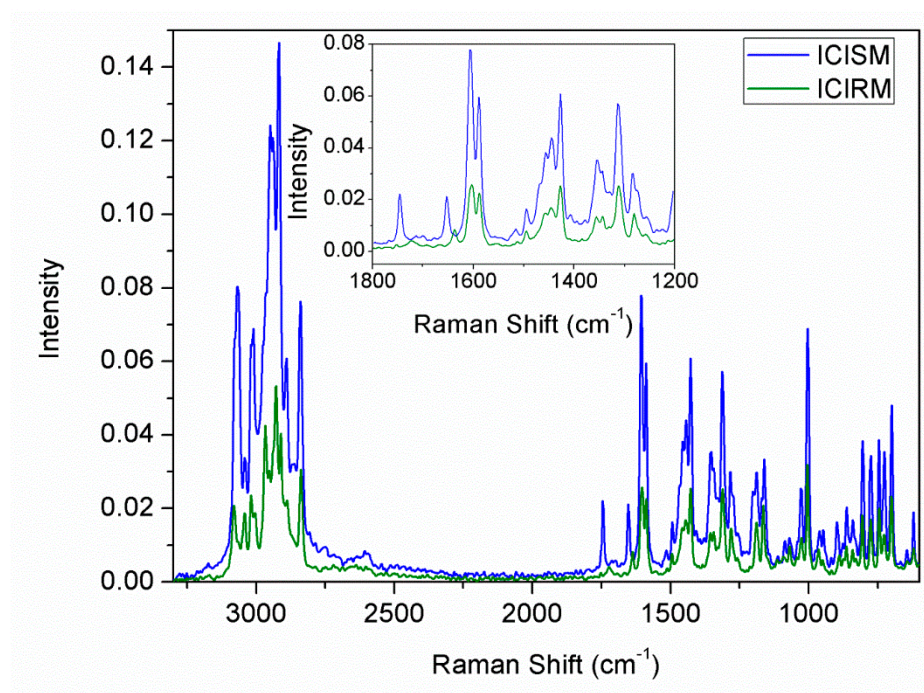


Figure S14. Comparison of Raman spectra of ICISM (blue) and ICIRM (green).

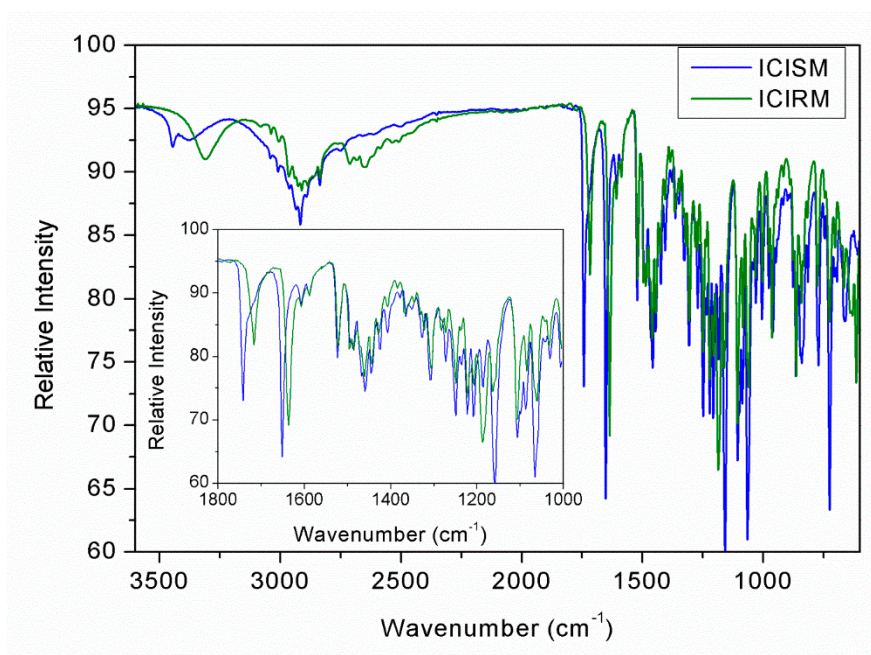


Figure S15. Comparison of IR spectra of ICISM (blue) and ICIRM (green).

IV. In Situ Granulation Experiment

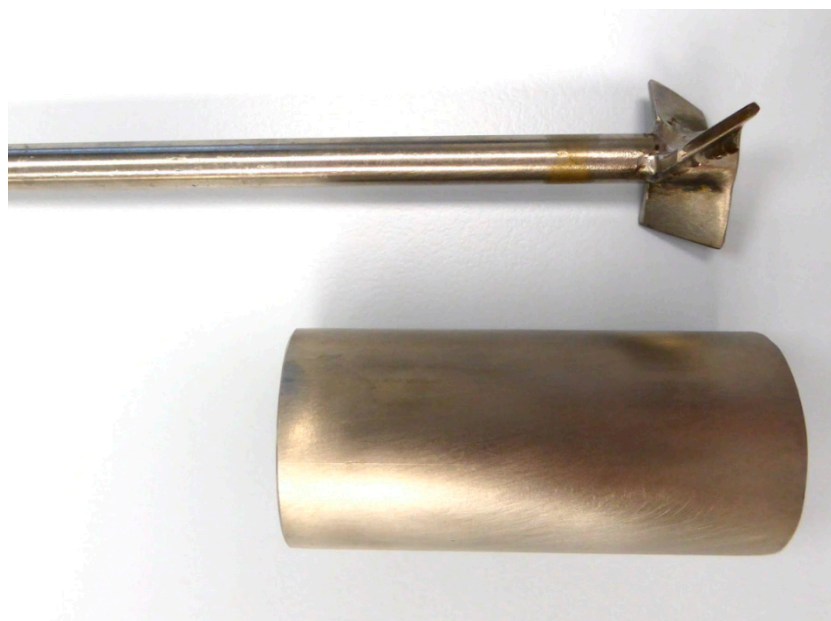


Figure S16. In-house small-scale high-shear granulator.

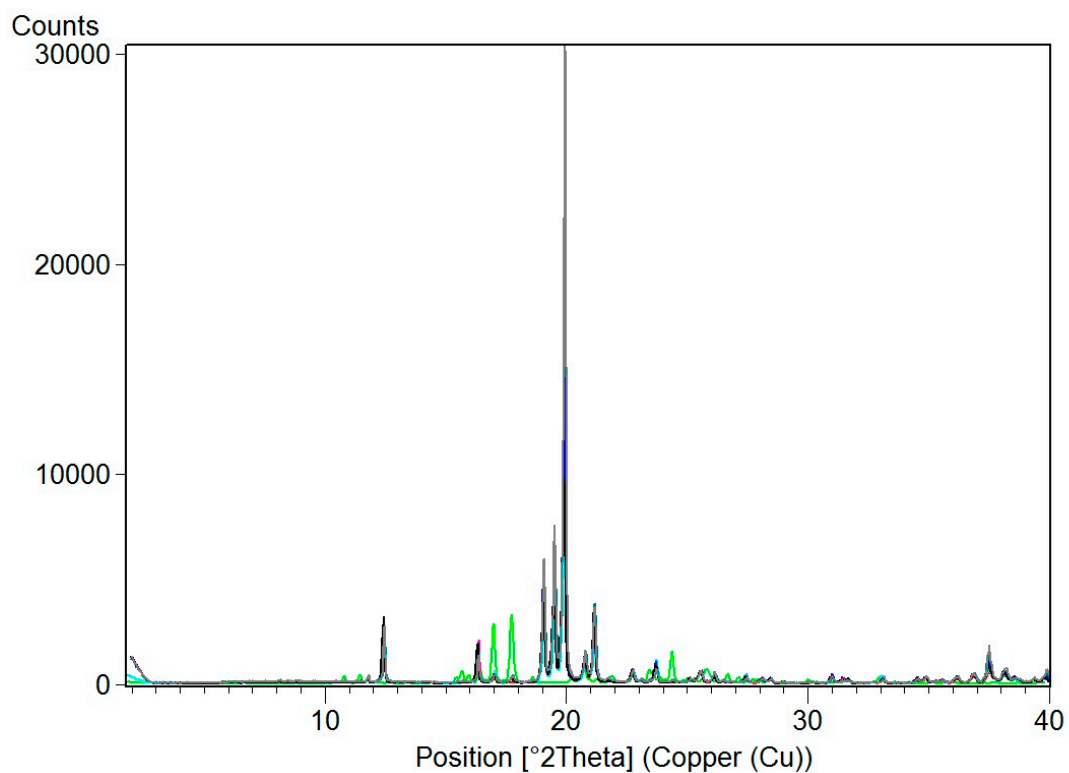


Figure S17. The XRPD patterns of pure ICISM (green) and granulation mixtures with lactose monohydrate.

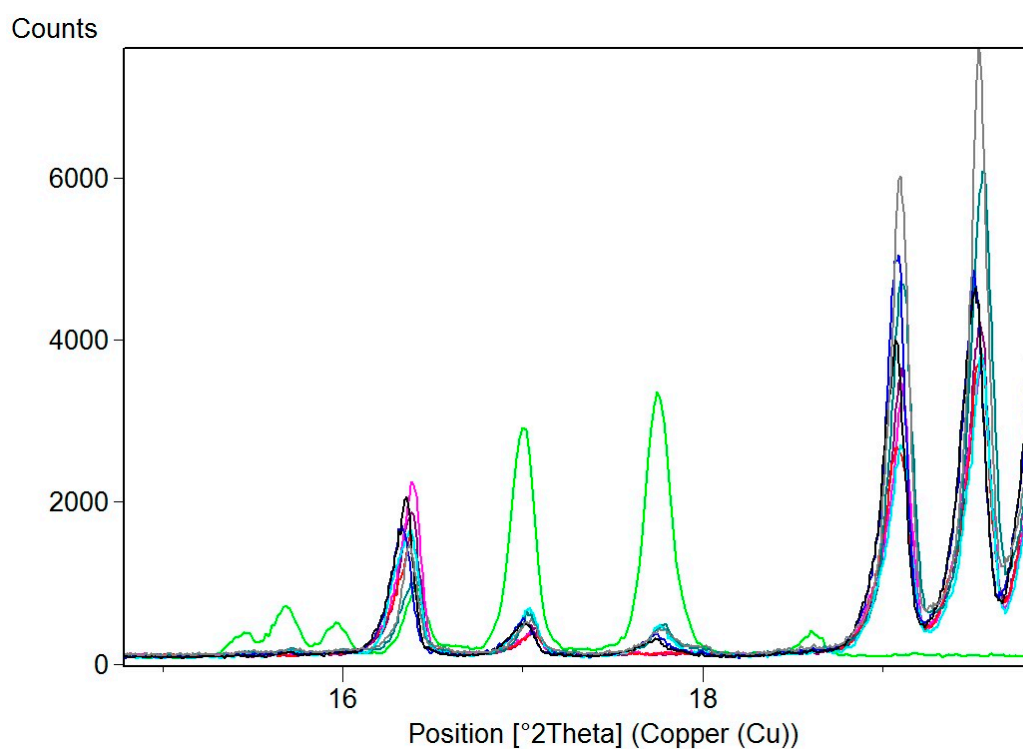


Figure S18. The detail of XRPD patterns of pure ICISM (green), ICISM + lactose monohydrate mixtures, and IVA HCl + (S)-mandelic acid + lactose monohydrate mixtures (red and magenta).

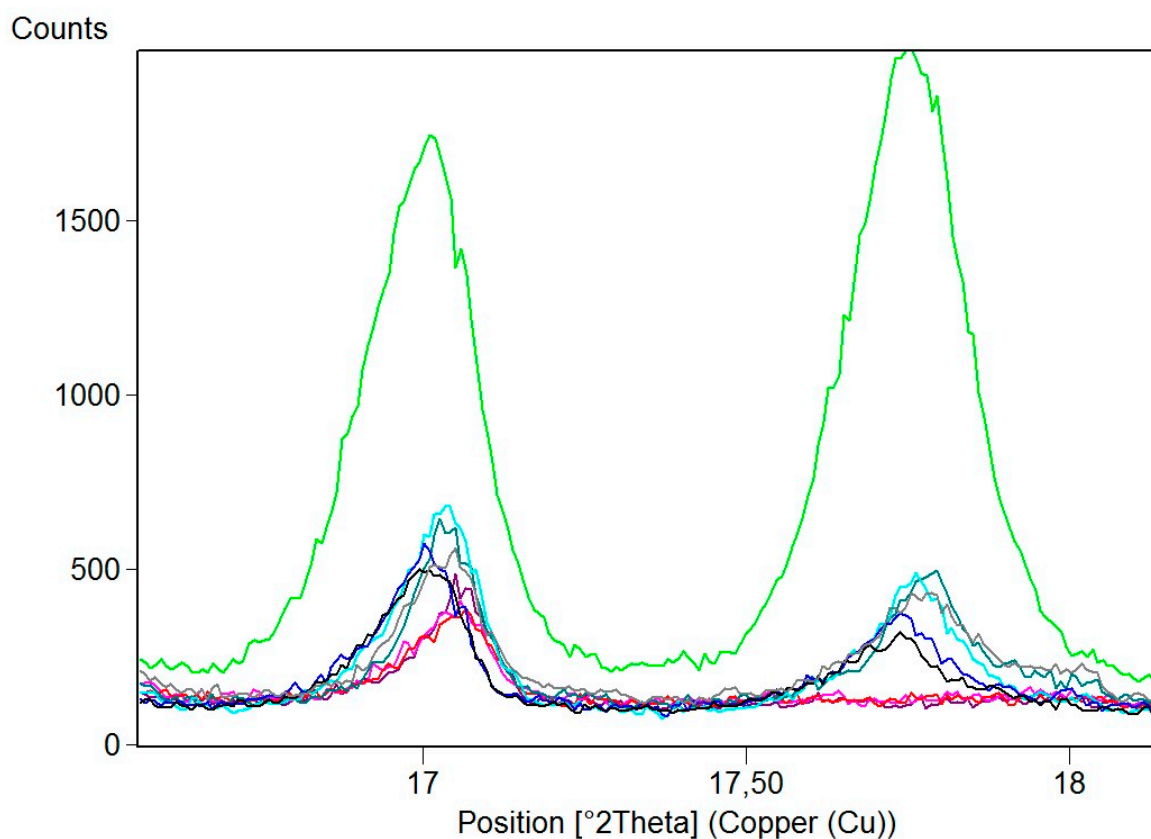


Figure S19. The detail of XRPD patterns of pure ICISM (green), ICISM + lactose monohydrate mixtures after granulation (black, blue, turquoise, grey, teal), and IVA HCl + (*S*)-mandelic acid + lactose monohydrate mixtures (red, violet, and magenta).

Figure 19 shows that the conversion of ivabradine hydrochloride and (*S*)-mandelic acid into ICISM co-crystal in the presence of lactose monohydrate occurred during wet granulation and that it could be observed by XRPD. Since lactose monohydrate overlaps peaks of ICISM, we had to find a window where peaks of the co-crystal would be clearly visible. The green pattern corresponds to pure ICISM. The other powder patterns correspond to wet granulation experiments where co-crystal was/was not successfully prepared in situ in the presence of lactose monohydrate. The conversion to co-crystal was also confirmed by ssNMR.